 doi:10.20944/preprints201810.0389.v2

Article

UAV based Crop Water Stress Index for wetland habitats as a meteorological drought indicator

Wojciech Ciężkowski[1,*], Sylwia Szporak-Wasilewska[2], Małgorzata Kleniewska[1], Jacek Jóźwiak[1], Tomasz Gnatowski[3], Piotr Dąbrowski[3], Maciej Góraj[1], Jan Szatyłowicz[3], Stefan Ignar[1] and Jarosław Chormański[1]

[1] Department of Hydraulic Engineering, Faculty of Civil and Environmental Engineering, Warsaw University of Life Sciences - SGGW, Nowoursynowska 166, 02-787 Warsaw, Poland; w.ciezkowski@levis.sggw.pl (W.C.); j.jozwiak@levis.sggw.pl (J.J.); malgorzata_kleniewska@sggw.pl (M.K.); m.goraj@levis.sggw.pl (M.G.); s.ignar@levis.sggw.pl (S.I.); j.chormanski@levis.sggw.pl (J.C.)

[2] Water Center Laboratory, Faculty of Civil and Environmental Engineering, Warsaw University of Life Sciences - SGGW, Nowoursynowska 166, 02-787 Warsaw, Poland; s-szporak@levis.sggw.pl

[3] Department of Environmental Improvement, Faculty of Civil and Environmental Engineering, Warsaw University of Life Sciences - SGGW, Nowoursynowska 166, 02-787 Warsaw, Poland; tomasz_gnatowski@sggw.pl (T.G.), piotr_dabrowski@sggw.pl (P.D.), jan_szatylowicz@sggw.pl (J.S.)

* Correspondence: w.ciezkowski@levis.sggw.pl; Tel.: +48-22-593-53-07 [1]

Abstract: Droughts which have been occurring more and more frequently in the recent years are usually associated with progressive climate changes. Modern monitoring methods are mainly associated with agricultural use due to the high market demand for services protecting against agricultural losses. In natural wetland ecosystems, this problem is neglected probably due to fact that those ecosystems are rich in water by definition. Nevertheless, wetlands as part of larger hydrological systems are subject to negative changes, such as droughts, which affect them to a varying degree. The good condition of wetland depends mainly on adequate hydration. Wetland hydrology determines the amount of nutrients entering and leaving a wetland, the chemistry of water and soil, the plants that grow in a wetland and its productivity. Deviation from optimal water supply conditions in a long-term perspective may lead to negative habitats changes. Therefore, this study is focused on the determination of Crop Water Stress Index (CWSI) as an indicator of water stress caused by drought for natural heterogeneous wetland habitats. CWSI calculations were based on remotely sensed land surface temperature and associated basic meteorological (air temperature and humidity) parameters. The performance of CWSI in selected wetland habitats (7140 and 7230 codes in Natura 2000 nomenclature) was confirmed by comparing the obtained values with hydrometeorological conditions (precipitation, temperature, vapour pressure deficit and groundwater level) and two drought indices (standardised precipitation index and standardised climatic water balance). The CWSI values show changes in the condition of plants caused by water stress. However, the exact determination of drought level by CWSI on this type of wetland habitats needs further research and this research is an initial point of using the LST based method for monitoring natural heterogeneous ecosystems vulnerable to ongoing climate changes and other threats that cause changes in their hydrological conditions.

Keywords: CWSI, Natura 2000, thermal remote sensing, wetlands, land surface temperature

1. Introduction

Droughts which have been occurring more and more frequently in the recent years are usually associated with progressive climate changes [1–5] and cause serious damage to the environment as well as the economy. As these phenomena are becoming increasingly intense covering larger and larger areas, a lot of attention is paid to them in scientific works, which leads to the development of new tools and methods designed to identify droughts. A key element in the decision-making process aimed at avoiding or reducing the effects of droughts is their monitoring [6–8]. Various types of

Preprints (www.preprints.org) | NOT PEER-REVIEWED | Posted: 23 November 2018 doi:10.20944/preprints201810.0389.v2

drought can be distinguished: meteorological, agricultural and hydrological. They are focused on different distinguishing factors, albeit they share the trait of observable impact on habitats – deterioration of the condition of plants.

The development of modern monitoring methods is mainly associated with agricultural use due to the high market demand for services protecting against agricultural losses. So far, no extensive research has been carried out in wetland areas particularly susceptible to changes in their water balance, which is probably due to the fact that wetland habitats are ecosystems rich in water by definition, while the groundwater level on such sites should remain close to the soil surface throughout the whole year. However, ongoing climate changes entail plant water stress that has a negative effect on the productivity and condition of crops and natural habitats; this becomes an increasing problem of wetlands, whose good condition depends on adequate hydration, while plant stress associated with drying results directly from the disturbance of groundwater level in the peat where they are formed. The disturbance of these conditions mainly by lowering of the water level leads to the peat subsidence due to changes of the physical conditions and mineralisation of organic matter by enhanced rates of microbial decomposition [9]. These processes have caused the reduction of peat porosity [10,11], which consequently results in a process of degradation of the habitat associated with the disappearance of plants species characteristic e.g. for alkaline fens (Natura 2000 - habitat 7230), such as *Valeriana simplicifolia, Epipactis palustris, Eleocharis quinqueflora*, as well as mosses such as *Limprichtia cossonii* and *Campylium stellatum*, or, in the case of transition mires and quaking bogs (Natura 2000 - habitat 7140), the plant species of *Scheuchzerietalia palustris* order, *Caricetalia nigrae* order, *Scheuchzerio-Caricetea* class - *Comarum palustre, Eriophorum angustifolium*, etc. These processes also consequently results in the reduction of the wetlands water capacity and the increase in air content in soil and its temperature result in increased CO_2 emission to the atmosphere [12,13]. Wetlands in good condition are ecosystems fulfilling an important function in larger hydrological systems as regulators of water circulation, for which the important water balance elements include snow retention [14], flood retention [15–17], evapotranspiration [18] and interception [19,20]. Their disturbance, resulting from the impact of progressive climate changes on the natural environment [21], has a significant impact on reducing the water retention of the catchment. Furthermore, the protection of wetlands constitutes the subject of multiple international conventions (e.g. Ramsar Convention on Wetlands), or directives (e.g. Bird and Habitat Directives, as the foundation of the European Natura 2000 nature protection system). The development of the best methods for identifying the risk of drying in wetland areas in the presence of climate change or other hazards causing changes in hydrological conditions (e.g. drainage) using modern remote sensing techniques is being expected by stakeholders responsible for maintaining a positive water balance and/or protection and management of the natural environment of wetlands. Due to the strong relationship between soil moisture content and the surface temperature, thermal remote sensing exhibits a large potential for the identification of the habitat water stress [22–24].

There are multiple indices used to identify and assess the intensity of a drought, and their characteristics and classifications are available in the literature [6,25–29]. For example, in the case of a meteorological drought [25], several methods are known, such as: Standardised Precipitation Index - SPI [30–33], Relative Precipitation Index - RPI [6], Effective Drought Index - EDI [34–36], Climatic Water Balance [6] and Standardised Climatic Water Balance - CWB and SCWB [37].

In order to assess the occurrence and intensity of an agricultural drought [38], the following indices are used, among others: Soil Moisture Index [39] or Crop Water Stress Index [40], with wide application possibilities [41], e.g. in determining the needs of irrigation of agricultural and horticultural crops [42,43]. The wide range of the CWSI application in addition to agricultural crops, includes its use to assess the water status of trees: fruit orchards [44,45], olive [46], and almond trees [47].

The main purpose of this study is the application of high-resolution thermal images from the UAV (Unmanned Aerial Vehicle) platform to determine CWSI (Crop Water Stress Index) on Natura 2000 habitats with codes 7140 (transition mires and quaking bogs) and 7230 (alkaline fens) in Poland. The CWSI was originally developed in the area of agricultural crops [48]; therefore, to check the possibility of using CWSI as a drought indicator for natural ecosystems in the temperate climate zone,

Preprints (www.preprints.org) | NOT PEER-REVIEWED | Posted: 23 November 2018 doi:10.20944/preprints201810.0389.v2

the CWSI values were compared with hydrometeorological parameters (precipitation, temperature, vapour pressure deficit and groundwater level) and two drought indices (Standardised Precipitation Index, Standardised Climatic Water Balance) widely used in Poland. The presented results show the overall possibility of using CWSI for wetland habitats, and it is noteworthy that no previous studies were conducted on this subject matter.

2. Materials and Methods

2.1. Study sites

The research was conducted on two semi natural habitats of Natura 2000 (Figure 1). The research of habitat 7230 (alkaline fens) was carried out in the Biebrza National Park area located in north-eastern Poland during vegetation season of 2016 . The research of habitat 7140 (transition mires and quaking bogs) was carried out in the Janów Forest Landscape Park area in south-eastern Poland during the vegetation season of 2017.

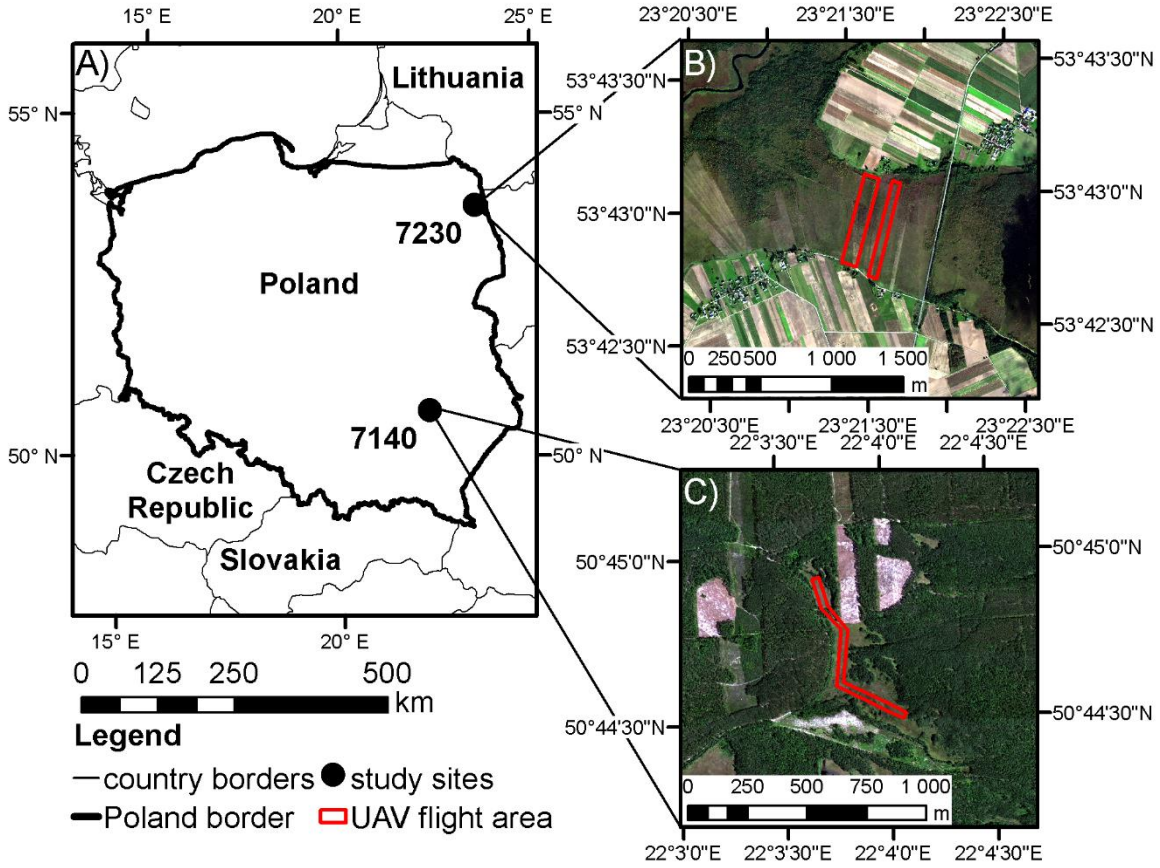

Figure 1. Study site location: A) location of study areas in Poland, B) UAV flight areas for habitat 7230 in the Biebrza National Park, C) UAV flight area for habitat 7140 in the Janów Forest Landscape Park

2.1.1. Biebrza National Park (Habitat 7230)

Research for habitat 7230 was carried out in the Upper Biebrza Valley in the area of Biebrza National Park (Figure 1B). The Upper Biebrza Valley is a north-eastern part of the Biebrza Proglacial Stream Valley which together with sandurs adjoining from the north currently constitutes the largest lowering of north-eastern Poland with a length of approx. 150 km and an area exceeding 2600 km^2. The Proglacial Stream Valley constitutes the largest complex of natural peatlands in Central Europe. In relation to the adjacent areas, it has different thermal and humidity characteristics of the air. This is due to the overlap of climate features associated with the vast areas of peatlands and the main

Preprints (www.preprints.org) | NOT PEER-REVIEWED | Posted: 23 November 2018 doi:10.20944/preprints201810.0389.v2

features of north-eastern Poland's climate, with an average annual temperature of 6 -7 °C (1971-2000) [49]. The average annual precipitation from the multiannual term of 1971-2000 is 550-600 mm in this area [49], while the duration of the snow cover lasts from 90 to 110 days. The research was carried out in the area near the Szuszalewo village characterised by extensively exploited alkaline peatlands, currently one of the most endangered natural habitats in Europe [50]. In the case of the alkaline peatlands, the groundwater level usually remains at or slightly above the ground surface in optimal conditions. The habitat is characterised by low fertility and high content of calcium ions. The dominant types of vegetation are moss-sedge communities (*Scheuchzerio-Caricetea nigrae* community) characterised by a large floral richness with a large share of rare and protected species, such as *Liparis loeselli*, or plant species from *Menyantho trifoliatae-Sphhagnetum teretis*, *Caricion davallianae*, *Caricetum rostratae*, and *Caricetum paniceo-lepidocarpae* communities. A very important group of plants within habitat 7230 are mosses, part of which are glacial relics. Changes in water relations, as well as succession towards forest and shrub communities, pose the greatest threat to the habitat.

2.1.2. Janów Forest Landscape Park (7140)

Research for habitat 7140 was carried out in the Janów Forest Landscape Park, which, together with the neighbouring Solska Wilderness, is one of the largest forest complexes in Poland (Figure 1C). According to the physiographic division of Poland [51], this area is located in the mesoregion of the Biłgoraj Plain called Puszczańska, which is a part of the Sandomierz Basin. The studied area lies in the Lublin district [52], relatively warm, with an average annual air temperature of 7-8 °C (1971-2000) [49]. The average annual precipitation amounts to 550-600 mm (1971-2000) [49], while the time of snow cover deposition amounts to 80-90 days. The area of the Janów Forest Landscape Park mainly consists of forest habitats, where the largest area is occupied by mixed wet coniferous forest and fresh coniferous forest. Aquatic-peat and aquatic communities are characterised with the greatest floristic richness. Habitat 7140 (transition mires and quaking bogs), within which the research was carried out, constitutes approximately 400 ha of the area of the Janów Forest Landscape Park. They are mainly peat-filled no-runoff land lowerings with a groundwater level arranged in optimal conditions at or slightly above the ground surface. Vegetation primarily consists of a moss and herbaceous layer, where the moss layer is composed mainly of *Sphagnum* moss and *Bryopsida*. Usually, one or two species of plants predominate in the habitat. In the Janów Forest Landscape Park, there are species of plants from *Eriophoro angustifolli-Sphagnetum recurvii, Caricetum rostratae, Caricetum lasiocarpae, Eriophorum vaginatum-Sphagnum fallax* or *Rhynchosporetum albae* communities. Changes in hydrological conditions, as well as trees and shrubs encroachment into open wetland areas in the conditions of lowering the groundwater level, pose the greatest threat to habitat 7140.

2.2. UAV aquisition and processing

Land surface temperature (LST) was recorded using a thermal camera installed on the UAV platform in 3 field campaigns in Biebrza National Park and 5 campaigns in Janów Forest Landscape Park (Table 1). The UAV platform was based and constructed on the DJI S1000+ frame (DJI, China) equipped with PIXHAWK autopilot (3D Robotics, USA) having a built-in IMU (Inertial Measurement Unit) system. GNSS navigation data was collected using Tersus-GNSS Precis BX306 GNSS device (Tersus GNSS China, China) enabling dual-frequency signal recording in both GPS and GLONASS systems. The Land Surface Temperature data logger was Optris PI640 radiometric camera (Optris GmbH, Germany) mounted on a 2-axis stabilising system. Additionally, in order to increase image interpretation possibilities manually select GCP (Ground Control Points) and an RGB images were recorded using UAV DJI Phantom 3 Professional platform (DJI, China).

Table 1. Acquisition dates and times, numbers of transect and flights per transect for both research areas.

Area	Date	Number of transect	Flights per transect	Time of flights
	24.07.2016	2	3	11:00-3:30

Preprints (www.preprints.org) | NOT PEER-REVIEWED | Posted: 23 November 2018 doi:10.20944/preprints201810.0389.v2

Biebrza National Park (7230)	07.09.2016		2	12:00-2:00
	18.09.2016		2	11:00-2:00
Janów Forest Landscape Park (7140)	14.07.2017	1	3	11:30-2:00
	01.08.2017		3	11:40-3:00
	19.07.2017		1	12:30
	30.08.2017		3	11:50-2:00
	09.09.2017		3	11:00-12:30

Flights over research transects were carried out autonomously along the planned routes, which ensured the repeatability of the area range that was acquired during subsequent flights. The set flight parameters allowed to obtain terrain resolution not worse than 10 cm/px. Air operations were carried out in possibly stable weather conditions. In addition, each time before starting the registration process, the camera was started for at least two minutes to stabilise the internal temperature of the device remaining under voltage. During recording, the device compensated the temperature changes of the sensor in intervals between 30 and 120 seconds through self-calibration.

Raw thermal data (saved as a video file) was converted into a radiometric form using Optris Pi Connect software (Optris GmbH, Germany). Subsequently, the individual frames of each recording were extracted. The process was carried out manually to ensure the quality of the obtained data (elimination of blurred images and saved at the time of self-calibration).

The coordinates of the projection centres of individual radiometric images were determined based on the GNSS on-board system recorded data. Then, the data set (the image-GPS position pair) was processed in Photoscan software (Agisoft LLC, Russia). The photogrammetric process consisted of generating a sparse point cloud, controlling the initially obtained model, creating a dense cloud of points, creating a DSM (digital surface model) and finally constructing an orthophotomosaic and exporting it to the TIFF format.

In addition, an orthophotomosaic in the visible band (RGB) was prepared for each of the research transects. The flight parameters were selected to obtain source data with a terrain resolution of 4.3 cm/px. In addition, a network of photogrammetric ground control points (N-GCP) was established in the study area. The coordinates of its individual points were measured using the GNSS RTK technique using GNSS receiver Topcon GRS-1 (Topcon, Japan) in real-time corrections with the TPI NetPRO network [53].

These points were used in the photogrammetric process to increase the internal coherence and external accuracy of the resulting orthophotomosaic. The obtained error of fitting on the matrix points did not exceed 3 px (regarding the resolution of the orthophotomosaic at the level of 5 cm/px).

The LST orthophotomosaic was subjected to final geometric rectification in the QGIS software based on characteristic points identifiable on the RGB orthophotomosaic. At least 20 points evenly distributed over the image were used per study area.

2.3. Meteorological data measuremnts

Meteorological data in the form of air temperature and relative humidity were measured using HOBO U23 Pro v2 Temperature/Relative Humidity Data Logger sensor (Onset®, USA). The temperature and relative humidity sensor was mounted at a height of 2 m, before the first UAV flight (between 9 and 10 a.m.) and removed after their completion (between 3 and 4 p.m.); the values were measured with a 10 minute time step. In addition, the temperature of the vegetation for Non-Water Stress baseline - NWSB determination was measured over an optimally moistened surface every 30 minutes using a non-contact infrared handheld OMEGA Os151-usb thermometer (OMEGA Engineering, INC).

2.4. CWSI calculations and hydrometeorological background

The CWSI was calculated according to the following equation [48,54]:

$$CWSI = (dT_m - dT_{LL}) / (dT_{UL} - DT_{LL}), \quad (1)$$

Preprints (www.preprints.org) | NOT PEER-REVIEWED | Posted: 23 November 2018 doi:10.20944/preprints201810.0389.v2

where dT – temperature difference between canopy (Tc) and air (Ta) and the subscripts m, LL and UL respectively refer to: the measured difference, lower (non-water-stressed) and upper limit of dT. Upper and lower limits of dT can be estimated based on the empirical [54] or the theoretical approach [48]. In this study, an empirical approach was used. It is based on the assumption that dT_{LL} is linearly related with Vapour Pressure Deficit (VPD) for non-water-stressed plants under specific climatic conditions - this relation is further referred to as Non-Water-Stressed Baseline (NWSB). Similarly, there is a linear relation between dT_{UL} and the Vapour Pressure Gradient (VPG) for the same plants when its transpiration is halted due to severe water stress. Upper and lower limits were calculated according to the following equations:

$$dT_{LL} = m \cdot VPD + b, \quad (2)$$

$$dT_{UL} = m \cdot VPG + b, \quad (3)$$

where "m" and "b" respectively refer to: slope and intercept of NWSB. VPG was estimated as the difference between the saturation vapour pressure at a given air temperature and the saturation vapour pressure at the air temperature elevated by factor "b".

The NWSB was developed for both investigated habitats based on field measurements of LST and meteorological parameters after significant precipitation according to the methodology described by [55].

Finally CWSI was calculated based on UAV LST data for whole transect. If more than one flight was carried out over the transect in a given period, the corresponding values of each map were averaged on the basis of all flights carried out over a given transect.

Based on the studies of the Institute of Meteorology and Water Management - National Research Institute - IMGW [56], the meteorological background of the study areas was analysed using temperature, relative humidyty and precipitation data from the nearest meteorological stations from year 1986-2017. Additionally, in both study areas, the level of groundwater was measured using Levelogger Model 3001 LT F15/M5 (Solnist Ltd. Canada). In the Janów Forest Landscape Park and in the Biebrza National Park, one piezometer was installed per study area. Data from piezometers was used as hydrological background for CWSI determination.

2.5. Drought indices

Two drought indices were calculated, based on meteorological data obtained from IMGW. The SPI and SCWB were selected as most valuable considering data access based on a review of popular meteorological drought indices.

The SPI was calculated according to the original methodology proposed by [30]. The SPI was calculated as the difference of precipitation from the mean for a specified time period divided by the standard deviation calculated from past records. For the calculation of SPI precipitation, data from 30 years back was used. The calculations were done for an averaging period equal to 3 months using a dedicated package in the R environment [57].

The SCWB is a standardised deviation of climatic water balance values in a given period by the mean long-term value of this period [58]. Climatic water balance is calculated as the difference between total precipitation and the reference evapotranspiration. For SCWB calculation, the reference evapotranspiration was calculated according to [59]. Decadal values of SCWB for a 30-year data series were calculated.

Classification of the SPI and SCWB values and meteorological drought category are presented in Table 2.

Table 2. Classification of meteorological drought according to SPI and SCWB values

Meteorological drought category	SPI values [30]	SCWB value [6]

Preprints (www.preprints.org) | NOT PEER-REVIEWED | Posted: 23 November 2018 doi:10.20944/preprints201810.0389.v2

mild drought	0 to -0.99	0.50 to -0.99
moderate drought	-1.00 to -1.49	
severe drought	-1.50 to -1.99	
extreme drought	≤ -2.00	

3. Results and discussion

In the first part of this chapter, the method of NWSB derivation used for CWSI calculation was presented and discussed. Then, CWSI spatial distribution within habitats borders was presented in the form of maps. To conclude the chapter, CWSI values were shown against different meteorological parameters as well as indices with a discussion of CWSI's performance as water stress indicator of wetland habitats.

3.1. Derivation of NWSB

The NWSBs for the examined habitats were obtained using an empirical approach [54] during days with optimal conditions for its derivation described by [60]. A linear function was fitted using the least squares method for habitat 7140 (equation 4) and a high coefficient of determination equal to 0.8 was achieved for VPD with values ranging from 0.5 to 2.0 kPa. Also, a linear function was fitted using the least squares method for habitat 7230 (equation 5) - coefficient of determination was lower, but still acceptable, equal to 0.65 for VPD, and ranged from 1.5 to 2.0 kPa. Using these NWSBs for VPDs outside of the mentioned ranges needs further work, especially for habitat 7230.

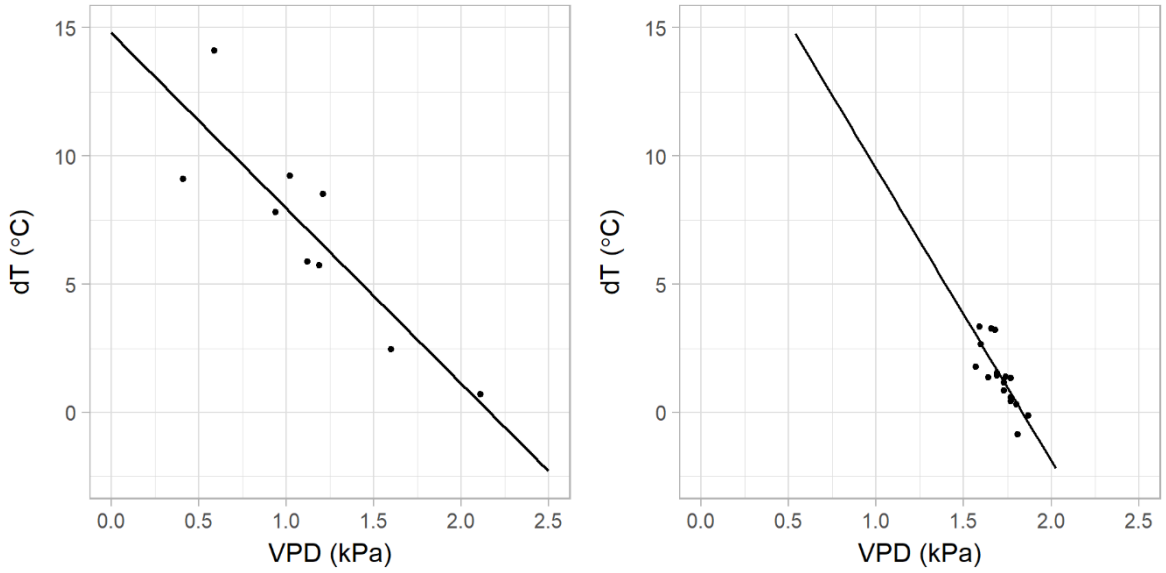

Figure 2. NWSB for habitat 7140 (left plot) and for habitat 7230 (right plot).

The NWSB for both of the examined habitats are shown in Figure 2. Equation 4 is NWSB for habitat 7140 based on measurements made in July after significant precipitation. Equation 5 is NWSB for habitat 7230 based on measurements made in July after significant precipitation.

$$dT = -7.14 \cdot VPD + 16.30,\ R^2 = 0.80, \quad (4)$$

$$dT = -11.63 \cdot VPD + 21.32,\ R^2 = 0.65 \quad (5)$$

In previous studies performed by other researchers, CWSI was calculated mainly for crops [42,48,54,55,61,62] also for: fruit orchards [44,63–65], olive trees [46] or almond trees [47]. The majority

Preprints (www.preprints.org) | NOT PEER-REVIEWED | Posted: 23 November 2018 doi:10.20944/preprints201810.0389.v2

of these studies were conducted in arid or semi-arid climate. No studies of CWSI in wetlands were found in literature, especially in temperate climate. Therefore, comparing the obtained parameters of NWSB with existing ones is infeasible.

3.2. CWSI maps

The map of the spatial distribution of CWSI values calculated in transects was presented in Figures 3 and 4, and on the boxplot prepared on the basis of 100000 randomly selected pixels from each map shown in subsequent sections. The significance of median differences in CWSI values between particular field campaigns in both areas was checked using the Kruskal-Wallis test in the R environment [66]. For both areas, differences in CWSI are significant at the level of $p < 0.05$.

The calculation results for the area of Janów Forest Landscape Park (Figure 3, Table 3) show low values (median equal to 0.02) of CWSI during the first measurement campaign (14.07.2017). Then, the CWSI values reach their maximum (median equal to 0.16) during the second measurement campaign (1.08.2017). Further, the values of the CWSI gradually decrease, reaching the minimum (median equal -0.04) during the last measurement campaign (09.09.2017). Lack of CWSI research in wetland habitats impede interpretation of obtained values. However, CWSI values lower than 0 were assumed to indicate non-water stress (optimal) condition. With this assumption on the days of 14.07, 30.08 and 09.09 studied habitats were in good (wet) condition. On 01.08 and 19.08 CWSI indicated that area suffered moderate water stress.

The spatial distribution of CWSI values in the first four campaigns showed lower values of CWSI in the southern part of the flight area, and in the fifth, nearly all of the area was characterised by CWSI values below 0 and the southern part did not stand out. In this part, few small ponds are located and the field assessment confirmed the better condition of plants in this region. Apart from the temporal pattern of water stress, CWSI also showed spatial variability in heterogeneous habitats and indicated parts of natural habitats that were less vulnerable to water stress caused by droughts.

Table 3. Statistics (minimum, median, maximum) of CWSI values for Janów Forest Landscape Park

date	CWSI (-)		
	minimum	median	maximum
14.07.2017	-0.29	0.02	0.26
01.08.2017	-0.06	0.16	0.33
19.08.2017	-0.19	0.13	0.44
30.08.2017	-0.23	0.03	0.33
09.09.2017	-0.27	-0.04	0.17

Preprints (www.preprints.org) | NOT PEER-REVIEWED | Posted: 23 November 2018 doi:10.20944/preprints201810.0389.v2

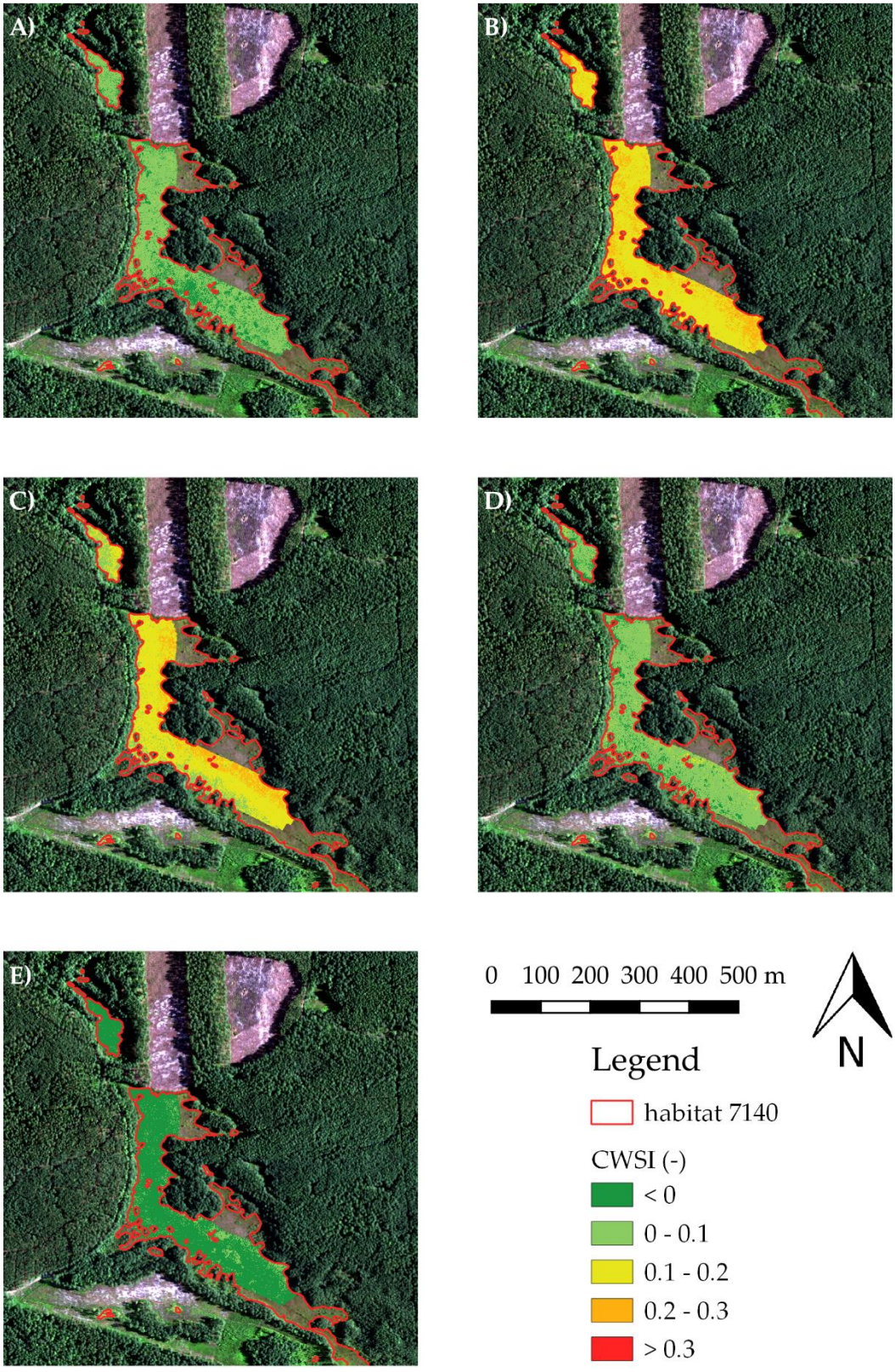

Figure 3. CWSI and habitat 7140 borders in the Janów Forest Landscape Park for 5 UAV campaigns: A) 14 July, B) 1 August, C) 19 August, D) 30 August, E) 9 September

 doi:10.20944/preprints201810.0389.v2

The CWSI calculation results for the Biebrza National Park (Figure 4, Table 4) showed the lowest values (median equal to -0.01) during the first measurement campaign (24.07.2016). In the next campaign on 07.09.2016, the median value remained equal to -0.01, but the maximum value was higher than in the first campaign. Further, the CWSI achieved the highest values (median equal to 0.03) in the research period. For this habitat the same threshold CWSI values were assumed, due to same reason. With this assumption, on 24.07 and 07.09, the measured area was in good, non-water stress condition. On 15.09, CWSI indicated that the area suffers from water stress.

The spatial distribution of CWSI values in the second and third campaign showed higher values of CWSI in the northern part of the two studied transects and the western part of the west transect. This part of the habitat was mowed just before the second field campaign. Hence, higher values of CWSI were observed. In the second campaign, the differences are less significant than during the third because the habitat was freshly mowed and just after high precipitation (Figure 6) its still evapotranspirates. The results showed a visible spatial pattern of the plant condition through spatial differences of CWSI values.

Table 4. Statistics (minimum, median, maximum) of CWSI values for Biebrza National Park

date	CWSI (-)		
	minimum	median	maximum
24.07.2016	-0.09	-0.01	0.06
07.09.2016	-0.09	-0.01	0.09
15.09.2016	-0.04	0.03	0.14

Preprints (www.preprints.org) | NOT PEER-REVIEWED | Posted: 23 November 2018 doi:10.20944/preprints201810.0389.v2

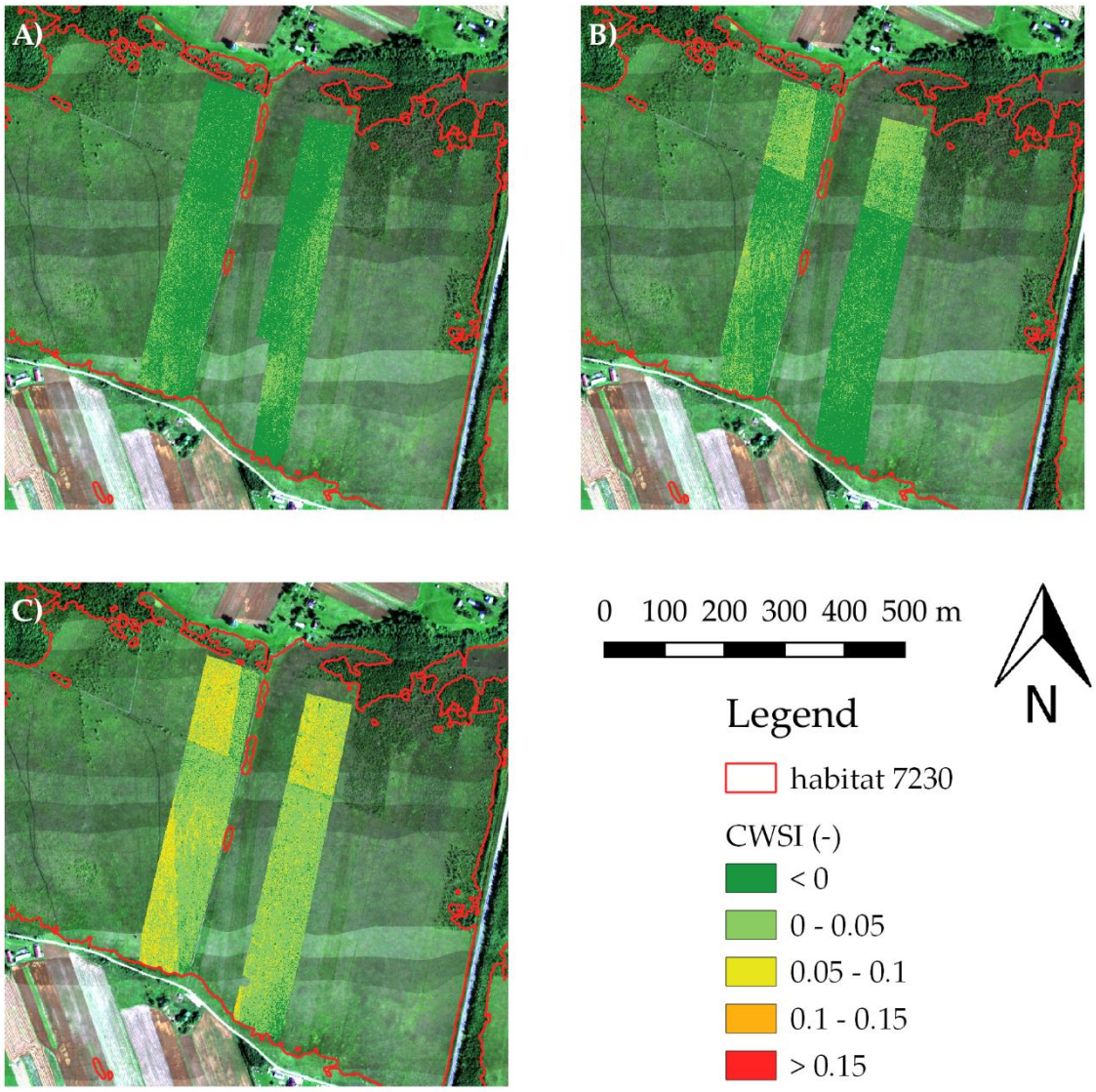

Figure 4. CWSI and habitat 7230 borders in the Biebrza National Park for 3 UAV campaigns in 2016: A) 24 July, B) 7 September, C) 15 September

3.3. CWSI and hydrometeorological parameters

The CWSI distribution (in form of boxplots) was presented against hydrometeorological parameters (precipitation, temperature, vapour pressure deficit and groundwater level) in Figure 5 for the Janów Forest Landscape Park, and in Figure 6 for the Biebrza National Park.

Assuming a CWSI value equal to 0 as a threshold value for a non-water-stress condition for examined habitats, in the Janów Forest Landscape Park, at the first and fourth field campaigns, a relatively moderate water-stress was indicated by CWSI (Figure 5). At the second and third field campaigns, the CWSI values indicated water-stress. At the fifth campaign, a major part of the studied area was in non-water stress condition. The habitat condition described by CWSI values is consistent with the observed hydrometeorological conditions. The first field campaign was conducted few days after a longer rainy period (one week with a daily precipitation sum between 1 to 5 mm), the groundwater level was relatively deep at 42 cm; this condition corresponds to the observed moderate water-stress. The second field campaign took place 2 weeks after precipitation on a day with

Preprints (www.preprints.org) | NOT PEER-REVIEWED | Posted: 23 November 2018 doi:10.20944/preprints201810.0389.v2

relatively high temperature and vapour pressure deficit. Such conditions caused the highest water-stress in this area. The third campaign took place on a day with the lowest groundwater level, but other meteorological parameters (temperature and vapour pressure deficit were lower than in the previous campaign; also, a few days without precipitation preceded this campaign) caused lower mean CWSI values. After the third field campaign, a rainy period started, which caused an increase in the groundwater level. With the decrease in temperature and vapour pressure deficit, these conditions caused a decrease in CWSI values. These results show that CWSI values correspond to hydrometeorological conditions. When the groundwater level, temperature and water pressure deficit indicated drier conditions, CWSI values also increased. Furthermore, the results show that CWSI is not affected by phenological changes. At the last field campaign in September (which is the end of the vegetation season), the lowest values of CWSI were observed after a significant rainfall period (5 days with high precipitation sum).

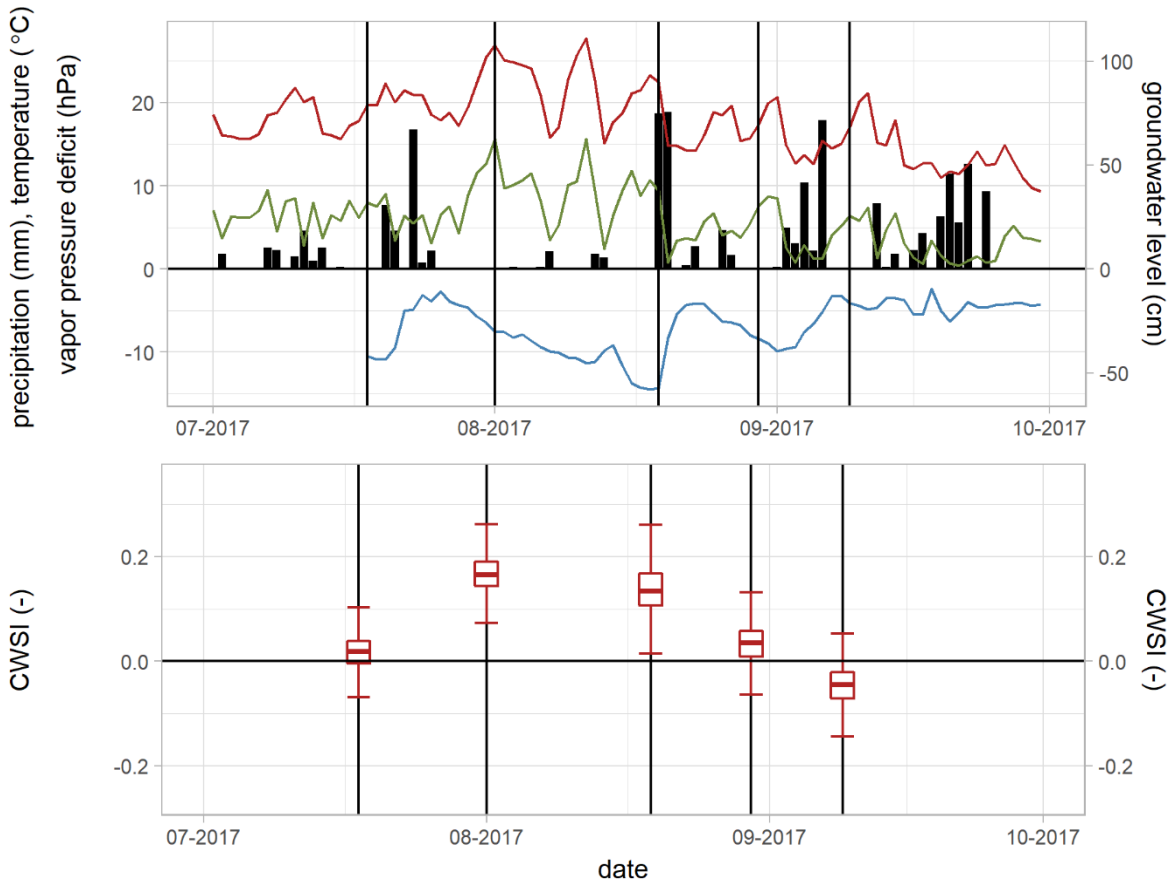

Figure 5. Precipitation (top panel black bars), temperature (top panel red line), vapour pressure deficit (top panel green line), groundwater level (top panel blue line) and CWSI distribution (bottom panel red boxplot which shows the median, the lower and upper hinges corresponds to the first and third quartiles, the upper and the lower whisker is 1.5 interquartile range) for Janów Forest Landscape Park, vertical black lines indicates UAV flights campaigns (Table 1).

In the Biebrza National Park (Figure 6) in the first field campaign majority of CWSI values were below 0 indicating non water-stress condition. In the next campaign, the mean CWSI value was higher but still, a major part of the research area was characterised by values below 0. In the last field campaign, a significant increase of CWSI values was observed and a major part of the research area was characterised by CWSI values indicating water stress. The habitat condition described by CWSI values is consistent with the observed hydrometeorological conditions. The first field campaign was conducted a week after the rainy period when groundwater level stabilised at around 15 cm below ground surface. After the first campaign, a rainy period started (lasting one month), in which the groundwater level was stabilised at around 10 cm below the ground surface. Later (after the 20th of

Preprints (www.preprints.org) | NOT PEER-REVIEWED | Posted: 23 November 2018 doi:10.20944/preprints201810.0389.v2

August), a decrease in the groundwater level was observed, caused by precipitation-free conditions. At the beginning of September, two days with high precipitation sum occurred and caused an increase in the groundwater level. After that, a previous decreasing trend in the groundwater level was observed. Two days after the mentioned high precipitation, the second campaign took place. The observed CWSI values indicated non-water stress conditions in a major part of the research area. A week later in the third campaign, CWSI values indicated water stress in a major part of the research area. These results shows that CWSI values corresponds to hydrometeorological conditions. Furthermore, the results show that CWSI is not affected by phenological changes. At the second field campaign in September (which is the end of the vegetation season), low values of CWSI were observed after significant rainfall (days with 8 and 22 mm of precipitation respectively).

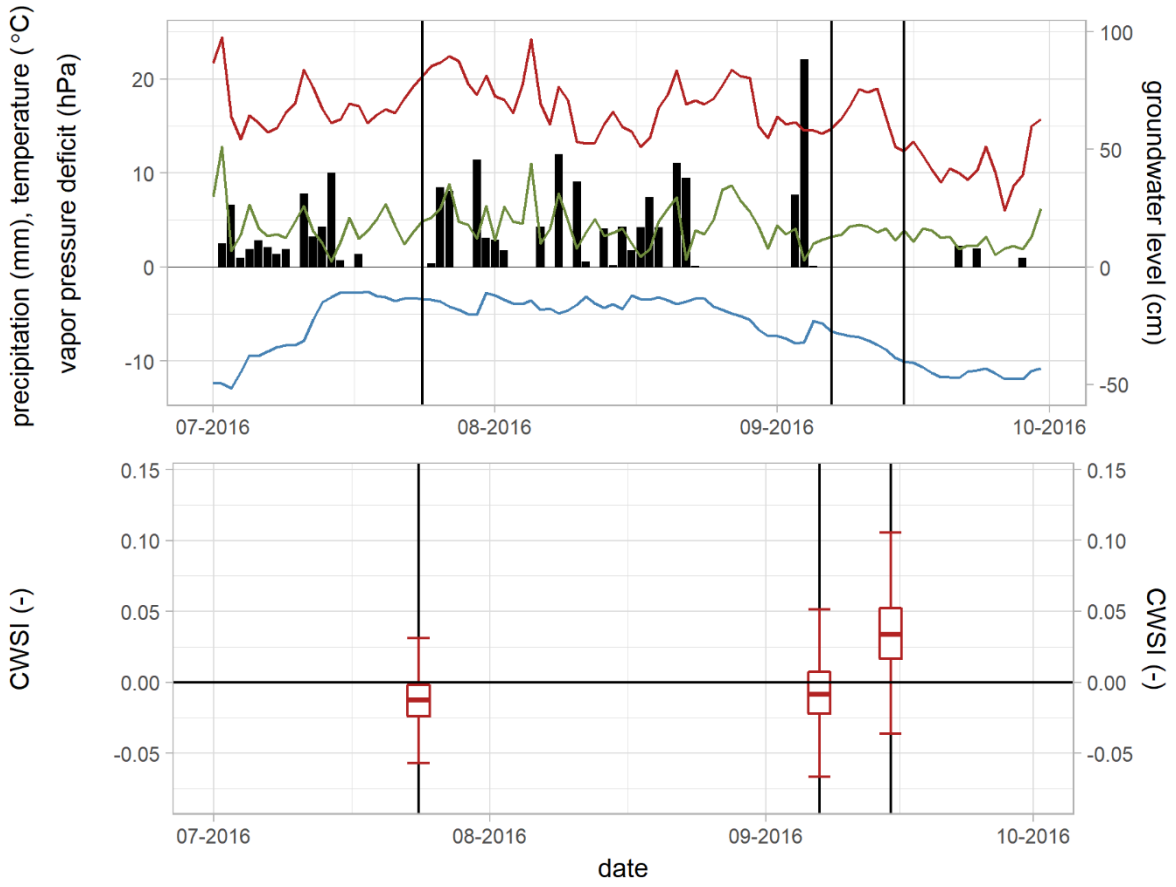

Figure 6. Precipitation (top panel black bars), temperature (top panel red line), vapour pressure deficit (top panel green line), groundwater level (top panel blue line) and CWSI distribution (bottom panel red boxplot which shows the median, the lower and upper hinges correspond to the first and third quartiles, , the upper and the lower whisker is 1.5 interquartile range) for Biebrza National Park, vertical black lines indicate UAV flight campaigns (Table 1).

3.4. CWSI against drought indicies

The CWSI distribution (in form of boxplots) was presented against SPI and SCWB in Figure 7 for both study sites.

Changes in CWSI values in the Janów Forest Landscape Park (Figure 7A) correspond with changes in SPI and SCWB. The highest values of CWSI (second field campaign) occurred when both drought indices showed mild drought. The third field campaign took place after a period of mild drought shown by SPI. But, in the day of the field campaign, after UAV flights, nearly 20 mm of rain fell (Figure 5), which resulted in an increase of SPI on this day and SCWB in this decade; however, CWSI still correctly indicated the water stress. In the fourth field campaign, CWSI values are mainly above 0, the SPI indicated no drought during this field campaign, and the SCWB was on the edge between mild and no drought. In the last field campaign, CWSI values were below 0 and both

Preprints (www.preprints.org) | NOT PEER-REVIEWED | Posted: 23 November 2018 doi:10.20944/preprints201810.0389.v2

drought indices showed no drought. These results show the overall agreement of CWSI and selected drought indices' courses. The results for the third field campaign showed that different approaches that are used in the calculation of indices cause interpretation issues. CWSI is calculated based on LST in point of time (in this case before rainfall), while SPI and SCWB are based on meteorological data from a given day or decade as well as conditions in the period before. These results showed that for 7140 habitat, the CWSI value c.a. 0 is a threshold of water stress and no water-stress condition. However, more studies on this habitat need to be done to specify the exact threshold values for different phases of droughts.

Changes in CWSI values in the Biebrza National Park (Figure 7B) correspond with changes in SCWB directly. The first and second field campaigns took place when values of SCWB indicated no droughts and CWSI values in this campaigns were mainly below 0. In the third field campaign, SCWB indicated mild drought and CWSI value increased to values above 0. Besides the first field campaign, SPI values confirmed the conditions described by CWSI. In the second field camping, SPI values were on the edge between drought and non-drought conditions, and CWSI values were mainly below 0. In the third field campaign, SPI values showed mild drought and CWSI values increased and indicated water-stress. SPI values during the first field campaign indicated mild drought, while CWSI values were below 0. This might be caused by the fact that habitat 7230 retained groundwater during spring, and with non-optimal meteorological conditions, plants were able to develop properly without indicating water-stress. These results showed that for this habitat, the CWSI value c.a. 0 is a threshold of water stress and no water-stress conditions. However, more studies on this habitat need to be done to specify the exact threshold values for different phases of droughts.

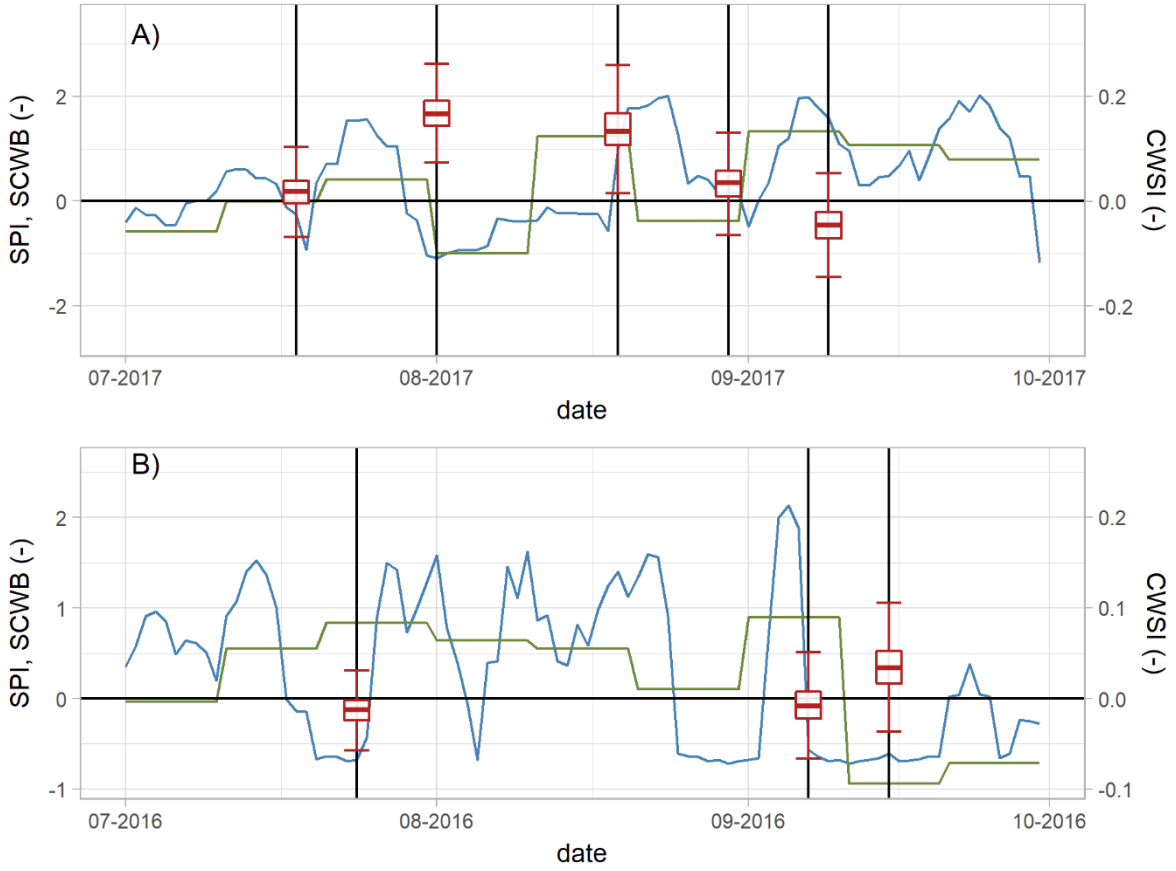

Figure 7. Drought indices: SPI (blue line) and SCWB (green line) and CWSI distribution (red boxplots which show the median, the lower and upper hinges correspond to the first and third quartiles, the upper and the lower whisker is 1.5 interquartile range) for the Janów Forest Landscape Park (top panel) and for the Biebrza National Park (bottom panel), vertical black lines indicates UAV flights campaigns (Table 1).

4. Conclusions

This study allowed to develop NWSB for two wetland habitats: 7140 (transition mires and quaking bogs) and 7230 (alkaline fens) in Natura 2000 nomenclature). The NWSB for habitat 7140 was developed in varied conditions (VPD ranged from 0.5 to 2.0 kPa). The NWSB for habitat 7230 was developed in more stable conditions (VPD ranged from 1.5 to 2.0 kPa). Hence, further research should be conducted in these habitats in order to confirm these results and the described CWSI on wetland more properly.

The CWSI calculations carried out on two wetland habitats (Natura 2000 code 7140 and 7230) together with the analysis of hydrometeorological conditions and two drought indices showed the possibility of using CWSI in wetland habitats as an indicator of water stress caused by drought. For both research areas, a temporal pattern of CWSI can be explained by changes in the hydrometeorological conditions. Also, the spatial distribution of CWSI on research areas properly indicated field conditions. In the southern part of the research area in Janów Forest Landscape Park, the CWSI values were low in all performed campaigns due to the local conditions (depression with limited water outflow). In the Biebrza National Park, the mowed part of the research area was characterised by high values of CWSI. This part was not exposed to water stress, but the main assumptions of CWSI method (difference in temperature of transpiring and non-transpiring plants) work the same.

Areas with a high proportion of *Sphagnum* mosses, which are the first to dry in unfavourable hydrometeorological conditions due to their way of growth leading to the formation of elevated clumps, are difficult to interpret. CWSI values in such conditions indicate that the habitat is drying within these clumps despite the fact that the measured values of soil moisture still remain high. In such situations, even a brief change in hydrometeorological conditions (e.g. intensive rainfall, high humidity, presence of dew) causes the clumps to saturate with water and *Sphagnum* mosses to quickly return to good condition. Only long-lasting and persisting unfavourable conditions can change this state both in the *Sphagnum* moss clumps and the entire habitat.

So far, most of the research on the application of CWSI (beyond that paper) was conducted in the areas of intensive agricultural use, in crop monocultures. The habitats analysed in this paper are heterogeneous with different plant communities in which the interpretation of the CWSI value often gave rise to some difficulties requiring insight into the species composition of individual research sites (e.g. high proportion of *Sphagnum* mosses and their sensitivity to changing hydrometeorological conditions against the soil moisture measurements). A detailed description of the drought process in wetlands with the use of CWSI, which is out of the scope of the paper, needs further research. It should focus on its relation with biophysical properties and functional plant treats in more diverse meteorological conditions. Due to uncertainty in natural conditions, field observation requires the preparation of a multi-sensor equipped site, or a laboratory experiment should be considered.

Author Contributions: Conceptualization, Jarosław Chormański; Data curation, Wojciech Ciężkowski, Sylwia Szporak-Wasilewska and Jacek Jóźwiak; Formal analysis, Wojciech Ciężkowski; Funding acquisition, Jarosław Chormański; Investigation, Wojciech Ciężkowski, Sylwia Szporak-Wasilewska, Małgorzata Kleniewska, Jacek Jóźwiak, Tomasz Gnatowski, Piotr Dąbrowski, Maciej Góraj, Jan Szatyłowicz and Jarosław Chormański; Methodology, Wojciech Ciężkowski, Sylwia Szporak-Wasilewska, Małgorzata Kleniewska, Jacek Jóźwiak, Tomasz Gnatowski, Piotr Dąbrowski, Maciej Góraj, Jan Szatyłowicz and Jarosław Chormański; Project administration, Stefan Ignar; Resources, Wojciech Ciężkowski and Jacek Jóźwiak; Software, Wojciech Ciężkowski; Supervision, Stefan Ignar and Jarosław Chormański; Validation, Wojciech Ciężkowski; Visualization, Wojciech Ciężkowski; Writing – original draft, Wojciech Ciężkowski; Writing – review & editing, Sylwia Szporak-Wasilewska, Małgorzata Kleniewska, Jacek Jóźwiak, Tomasz Gnatowski, Piotr Dąbrowski, Maciej Góraj, Jan Szatyłowicz and Jarosław Chormański.

Funding: This research was funded by the project HabitatARS (BIOSTRATEG2/297915/3/NCBR/2016). The innovative approach supporting monitoring of non-forest Natura 2000 habitats, using remote sensing methods financed by The National Centre for Research and Development.

Acknowledgments: The air temperature, relative humidity and precipitation were made available by the Institute of Meteorology and Water Management, National Research Institute (IMGW-PIB, https://dane.imgw.pl/)

Conflicts of Interest: The authors declare no conflict of interest

References

1. Spinoni, J.; Vogt, J. V; Naumann, G.; Barbosa, P.; Dosio, A. Will drought events become more frequent and severe in Europe? *Int. J. Climatol.* **2018**, *38*, 1718–1736.

2. Schubert, S. D.; Stewart, R. E.; Wang, H.; Barlow, M.; Berbery, E. H.; Cai, W.; Hoerling, M. P.; Kanikicharla, K. K.; Koster, R. D.; Lyon, B. Global meteorological drought: a synthesis of current understanding with a focus on SST drivers of precipitation deficits. *J. Clim.* **2016**, *29*, 3989–4019.

3. Trenberth, K. E.; Dai, A.; Van Der Schrier, G.; Jones, P. D.; Barichivich, J.; Briffa, K. R.; Sheffield, J. Global warming and changes in drought. *Nat. Clim. Chang.* **2014**, *4*, 17.

4. Dai, A. Drought under global warming: a review. *Wiley Interdiscip. Rev. Clim. Chang.* **2011**, *2*, 45–65.

5. Dai, A. Increasing drought under global warming in observations and models. *Nat. Clim. Chang.* **2013**, *3*, 52.

6. Łabędzki, L.; Bąk, B. Meteorological and agricultural drought indices used in drought monitoring in Poland: a review. *Meteorol. Hydrol. Water Manag. Res. Oper. Appl.* **2014**, *2*.

7. Funk, C. New satellite observations and rainfall forecasts help provide earlier warning of African drought. *Earth Obs.* **2009**, *21*, 23–27.

8. Svoboda, M.; LeComte, D.; Hayes, M.; Heim, R.; Gleason, K.; Angel, J.; Rippey, B.; Tinker, R.; Palecki, M.; Stooksbury, D. The drought monitor. *Bull. Am. Meteorol. Soc.* **2002**, *83*, 1181–1190.

9. Deverel, S. J.; Ingrum, T.; Leighton, D. Present-day oxidative subsidence of organic soils and mitigation in the Sacramento-San Joaquin Delta, California, USA. *Hydrogeol. J.* **2016**, *24*, 569–586.

10. Könönen, M.; Jauhiainen, J.; Laiho, R.; Kusin, K.; Vasander, H. Physical and chemical properties of tropical peat under stabilised land uses. *Mires peat* **2015**, *16*, 1–13.

11. Hewelke, E.; Szatyłowicz, J.; Gnatowski, T.; Oleszczuk, R. Effects of soil water repellency on moisture patterns in a degraded sapric histosol. *L. Degrad. Dev.* **2016**, *27*, 955–964.

12. Kluge, B.; Wessolek, G.; Facklam, M.; Lorenz, M.; Schwärzel, K. Long-term carbon loss and CO2-C release of drained peatland soils in northeast Germany. *Eur. J. Soil Sci.* **2008**, *59*, 1076–1086.

13. Mäkiranta, P.; Laiho, R.; Fritze, H.; Hytönen, J.; Laine, J.; Minkkinen, K. Indirect regulation of heterotrophic peat soil respiration by water level via microbial community structure and temperature sensitivity. *Soil Biol. Biochem.* **2009**, *41*, 695–703.

14. Berezowski, T.; Nossent, J.; Chormański, J.; Batelaan, O. Spatial sensitivity analysis of snow cover data in a distributed rainfall-runoff model. *Hydrol. Earth Syst. Sci.* **2015**, *19*, 1887–1904.

15. Chormanski, J.; Okruszko, T.; Ignar, S.; Batelaan, O.; Rebel, K. T.; Wassen, M. J. Flood mapping with remote sensing and hydrochemistry: A new method to distinguish the origin of flood water during floods. *Ecol. Eng.* **2011**, *37*, 1334–1349.

16. Keizer, F. M.; Schot, P. P.; Okruszko, T.; Chormański, J.; Kardel, I.; Wassen, M. J. A new look at the flood pulse concept: the (ir) relevance of the moving littoral in temperate zone rivers. *Ecol. Eng.* **2014**, *64*, 85–99.

17. Mirosław-Świątek, D.; Szporak-Wasilewska, S.; Grygoruk, M. Assessing floodplain porosity for accurate quantification of water retention capacity of near-natural riparian ecosystems—a case study of the Lower Biebrza Basin, Poland. *Ecol. Eng.* **2016**, *92*, 181–189.

18. Kleniewska, M.; Gołaszewski, D.; Majewski, G.; Szporak-Wasilewska, S.; Rozbicka, K.; Rozbicki, T. Diurnal Course of the Main Heat Balance Components of a Marshy Meadow in the Lower Biebrza River Valley. *Polish J. Environ. Stud.* **2015**, *24*.

19. Ciężkowski, W.; Berezowski, T.; Kleniewska, M.; Szporak-Wasilewska, S.; Chormański, J. Modelling wetland growing season rainfall interception losses based on maximum canopy storage measurements. *Water* **2017**, 10(1),

20. Berezowski, T.; Chormański, J.; Kleniewska, M.; Szporak-Wasilewska, S. Towards rainfall interception capacity estimation using ALS LiDAR data. In *Geoscience and Remote Sensing Symposium (IGARSS), 2015 IEEE International*; IEEE, **2015**; pp. 735–738.

21. Berezowski, T.; Wassen, M.; Szatyłowicz, J.; Chormański, J.; Ignar, S.; Batelaan, O.; Okruszko, T. Wetlands in flux: looking for the drivers in a central European case. *Wetl. Ecol. Manag.* **2018**, 26(5), 849--863.

22. Khanal, S.; Fulton, J.; Shearer, S. An overview of current and potential applications of thermal remote sensing in precision agriculture. *Comput. Electron. Agric.* **2017**, *139*, 22–32.

23. Anderson, M. C.; Hain, C.; Otkin, J.; Zhan, X.; Mo, K.; Svoboda, M.; Wardlow, B.; Pimstein, A. An intercomparison of drought indicators based on thermal remote sensing and NLDAS-2 simulations with US Drought Monitor classifications. *J. Hydrometeorol.* **2013**, *14*, 1035–1056.

24. Jones, H. G. Irrigation scheduling: advantages and pitfalls of plant-based methods. *J. Exp. Bot.* **2004**, *55*, 2427–2436.

25. Palmer, W. C. Meteorological drought. Research Paper No. 45. Washington, DC: US Department of Commerce. *Weather Bur.* **1965**, 59.

26. Heim Jr, R. R. A review of twentieth-century drought indices used in the United States. *Bull. Am. Meteorol. Soc.* **2002**, *83*, 1149–1165.

27. Vogt, J. V; Somma, F. (Eds.) Drought and drought mitigation in Europe. Advances in natural and technological hazards research, vol. 14. Kluwer Academic Publisher, Dordrecht, **2000**.

28. Hayes, M. J.; Alvord, C.; Lowrey, J. Drought indices. *Intermt. West Clim. Summ.* **2007**, *3*, 2–6.

29. Sepulcre-Canto, G.; Horion, S.; Singleton, A.; Carrao, H.; Vogt, J. Development of a Combined Drought Indicator to detect agricultural drought in Europe. *Nat. Hazards Earth Syst. Sci.* **2012**, *12*, 3519–3531.

30. McKee, T. B.; Doesken, N. J.; Kleist, J. The relationship of drought frequency and duration to time scales. In *Proceedings of the 8th Conference on Applied Climatology*; American Meteorological Society Boston, MA, **1993**; Vol. 17, pp. 179–183.

31. Bloomfield, J. P.; Marchant, B. P. Analysis of groundwater drought building on the standardised precipitation index approach. *Hydrol. Earth Syst. Sci.* **2013**, *17*, 4769–4787.

32. Paulo, A. A.; Pereira, L. S.; Matias, P. G. Analysis of local and regional droughts in southern Portugal using the theory of runs and the Standardised Precipitation Index. In *Tools for Drought Mitigation in Mediterranean Regions*; Springer, **2003**; pp. 55–78.

33. Guenang, G. M.; Kamga, F. M. Computation of the standardized precipitation index (SPI) and its use to assess drought occurrences in Cameroon over recent decades. *J. Appl. Meteorol. Climatol.* **2014**, *53*, 2310–2324.

34. Morid, S.; Smakhtin, V.; Moghaddasi, M. Comparison of seven meteorological indices for drought monitoring in Iran. *Int. J. Climatol. A J. R. Meteorol. Soc.* **2006**, *26*, 971–985.

35. Kim, D.-W.; Byun, H.-R.; Choi, K.-S. Evaluation, modification, and application of the Effective Drought Index to 200-Year drought climatology of Seoul, Korea. *J. Hydrol.* **2009**, *378*, 1–12.

36. Deo, R. C.; Şahin, M. Application of the extreme learning machine algorithm for the prediction of monthly Effective Drought Index in eastern Australia. *Atmos. Res.* **2015**, *153*, 512–525.

37. Tokarczyk, T. Classification of low flow and hydrological drought for a river basin. *Acta Geophys.* **2013**, *61*, 404–421.

38. Petrasovits, I.; others General review on drought strategies. In *Proceedings 14th International Congress on Irrigation and Drainage, Rio de Janeiro, Brazil.*; **1990**; pp. 1–11.

39. Baier, W. Concepts of soil moisture availability and their effect on soil moisture estimates from a meteorological budget. *Agric. Meteorol.* **1969**, *6*, 165–178.

40. Gardner, B. R.; Nielsen, D. C.; Shock, C. C. Infrared thermometry and the crop water stress index. I. History,

theory, and baselines. *J. Prod. Agric.* **1992**, *5*, 462–466.

41. Maes, W. H.; Steppe, K. Estimating evapotranspiration and drought stress with ground-based thermal remote sensing in agriculture: a review. *J. Exp. Bot.* **2012**, *63*, 4671–4712.

42. Irmak, S.; Haman, D. Z.; Bastug, R. Determination of crop water stress index for irrigation timing and yield estimation of corn. *Agron. J.* **2000**, *92*, 1221–1227.

43. Erdem, Y.; Erdem, T.; ORTA, A. H.; Okursoy, H. Irrigation scheduling for watermelon with crop water stress index (CWSI). *J. Cent. Eur. Agric.* **2006**, *6*, 449–460.

44. Andrews, P. K.; Chalmers, D. J.; Moremong, M. Canopy-air temperature differences and soil water as predictors of water stress of apple trees grown in a humid, temperate climate. *J. Am. Soc. Hortic. Sci.* **1992**, *117*, 453–458.

45. Wang, D.; Gartung, J. Infrared canopy temperature of early-ripening peach trees under postharvest deficit irrigation. *Agric. Water Manag.* **2010**, *97*, 1787–1794.

46. Berni, J. A. J.; Zarco-Tejada, P. J.; Sepulcre-Cantó, G.; Fereres, E.; Villalobos, F. Mapping canopy conductance and CWSI in olive orchards using high resolution thermal remote sensing imagery. *Remote Sens. Environ.* **2009**, *113*, 2380–2388.

47. García-Tejero, I. F.; Rubio, A. E.; Viñuela, I.; Hernández, A.; Gutiérrez-Gordillo, S.; Rodríguez-Pleguezuelo, C. R.; Durán-Zuazo, V. H. Thermal imaging at plant level to assess the crop-water status in almond trees (cv. Guara) under deficit irrigation strategies. *Agric. Water Manag.* **2018**, *208*, 176–186.

48. Jackson, R. D.; Idso, S. B.; Reginato, R. J.; Pinter Jr, P. J. Canopy temperature as a crop water stress indicator. *Water Resour. Res.* **1981**, *17*, 1133–1138.

49. Pogodynka. Avilable online: http://klimat.pogodynka.pl/pl/climate-maps/#Mean_Temperature/Monthly/2010/1/Winter (accessed on 14.11.2018)

50. Kopeć, D.; Michalska-Hejduk, D.; Berezowski, T.; Borowski, M.; Rosadziński, S.; Chormański, J. Application of multisensoral remote sensing data in the mapping of alkaline fens Natura 2000 habitat. *Ecol. Indic.* **2016**, *70*, 196–208.

51. Kondracki, J. *Geografia regionalna polski*; Wydawn. Naukowe PWN, 2000 (in Polish).

52. Kondracki, J. *Geografia fizyczna Polski*; Państ. Wydaw. Naukowe, 1978 (in Polish).

53. tpinet. Avilalble online: http://www.tpinet.pl (accessed on 14.11.2018).

54. Idso, S. B.; Jackson, R. D.; Pinter Jr, P. J.; Reginato, R. J.; Hatfield, J. L. Normalizing the stress-degree-day parameter for environmental variability. *Agric. Meteorol.* **1981**, *24*, 45–55.

55. Taghvaeian, S.; Chávez, J. L.; Hansen, N. C. Infrared thermometry to estimate crop water stress index and water use of irrigated maize in Northeastern Colorado. *Remote Sens.* **2012**, *4*, 3619–3637.

56. Biuletyn Monitoringu Klimatu Polski. Avilalbe online: http://old.imgw.pl/extcont/biuletyn_monitoringu (accessed on 14.11.2018).

57. Beguería, S.; Vicente-Serrano, S. M. SPEI: Calculation of the Standardised Precipitation-Evapotranspiration Index 2017.

58. Łabędzki, L.; Bąk, B. Standaryzowany klimatyczny bilans wodny jako wskaźnik suszy. *Acta Agrophysica* **2004**, *3*, 117–124 (in Polish).

59. Allen, R. G.; Pereira, L. S.; Raes, D.; Smith, M. Crop evapotranspiration-Guidelines for computing crop water requirements-FAO Irrigation and drainage paper 56. *FAO, Rome* **1998**, *300*, D05109.

60. Bellvert, J.; Zarco-Tejada, P. J.; Girona, J.; Fereres, E. Mapping crop water stress index in a 'Pinot-noir'vineyard: comparing ground measurements with thermal remote sensing imagery from an unmanned aerial vehicle. *Precis. Agric.* **2014**, *15*, 361–376.

61. DeJonge, K. C.; Taghvaeian, S.; Trout, T. J.; Comas, L. H. Comparison of canopy temperature-based water

 doi:10.20944/preprints201810.0389.v2

stress indices for maize. *Agric. water Manag.* **2015**, *156*, 51–62.

62. Amazirh, A.; Er-Raki, S.; Chehbouni, A.; Rivalland, V.; Diarra, A.; Khabba, S.; Ezzahar, J.; Merlin, O. Modified Penman--Monteith equation for monitoring evapotranspiration of wheat crop: relationship between the surface resistance and remotely sensed stress index. *Biosyst. Eng.* **2017**, *164*, 68–84.

63. Bellvert, J.; Marsal, J.; Girona, J.; Zarco-Tejada, P. J. Seasonal evolution of crop water stress index in grapevine varieties determined with high-resolution remote sensing thermal imagery. *Irrig. Sci.* **2015**, *33*, 81–93.

64. Bahmani, O.; Sabziparvar, A. A.; Khosravi, R. Evaluation of yield, quality and crop water stress index of sugar beet under different irrigation regimes. *Water Sci. Technol. Water Supply* **2017**, *17*, 571–578.

65. Park, S.; Ryu, D.; Fuentes, S.; Chung, H.; Hernández-Montes, E.; O'Connell, M. Adaptive estimation of crop water stress in nectarine and peach orchards using high-resolution imagery from an unmanned aerial vehicle (UAV). *Remote Sens.* **2017**, *9*, 828.

66. R Core Team R: A Language and Environment for Statistical Computing **2017.**